ELSEVIER

Journal of Molecular Catalysis A: Chemical 176 (2001) 253–265

JOURNAL OF MOLECULAR CATALYSIS A: CHEMICAL

www.elsevier.com/locate/molcata

Oxidative coupling of methane on $LaAlO_3$ perovskites partially substituted with alkali or alkali-earth ions

R. Spinicci [a], P. Marini [a], S. De Rossi [b], M. Faticanti [b], P. Porta [b,*]

[a] *Dipartimento di Energetica, Università di Firenze, V. S. Marta 3, 50139 Firenze, Italy*

[b] *Centro di Studio del CNR su "Struttura e Attività Catalitica di Sistemi di Ossidi" (SACSO), c/o Dipartimento di Chimica, Università "La Sapienza", Piazzale A. Moro 5, 00185 Rome, Italy*

Received 6 March 2001; accepted 16 May 2001

Abstract

Methane coupling was investigated at 600–750°C on $LaAlO_3$, $La_{1-x}M_xAlO_3$ (M = Na, K, Ca, Ba, $x = 0.1$) and $LaAl_{1-x}M_xO_3$ (M = Li, Mg, $x = 0.1$) perovskite-type catalysts, prepared by calcining the citrate precursors at 800°C for 5 h. The introduction of the alkali and alkali-earth metals produces oxygen vacancies and higher bond strength for both lattice and surface oxygen species. The substitution of Al^{3+} with Li^+ and Mg^{2+} increases both catalytic activity and selectivity to C_2-hydrocarbons in comparison with unsubstituted $LaAlO_3$ perovskite. A diffusional control is suggested for the oxidation to carbon oxides, whereas methane coupling should occur under kinetic control. The overall process should take place through a complex pattern of reactions. The results were rationalized on the basis of the structural properties of the catalysts and of their adsorptive behavior towards oxygen, investigated by means of temperature programmed desorption (TPD).

Keywords: La–Al perovskite oxides; Substituted perovskites; Methane coupling; Oxygen reactivity

1. Introduction

Direct and indirect methods are known for methane valorisation. The indirect routes are based mainly on the steam reforming to produce synthesis gas ($CO + H_2$) [1,2], which can then be converted to the desired liquid fuels. Since reforming is a highly energy consuming process, considerable efforts have been made for many years to develop direct conversion reactions producing partially oxidized compounds (mainly methanol) [3,4], and products (ethane and ethylene) derived from the oxidative coupling of methane [5,6].

Either the reactions of partial oxidation to methanol or the reaction of oxidative coupling to ethane and ethylene are highly exothermic and much favored from a thermodynamic point of view. However, the major difficulty to overcome in CH_4 conversion is the strength of the first C–H bond (435 kJ mol^{-1}). This implies that coupling occurs only at very high temperatures (≥700°C), with problems such as (i) occurrence of homogeneous gas-phase reactions [7] leading to a complex pattern of parallel reactions, (ii) kinetic stabilization of the product, with the possibility of a complex pattern of consecutive reactions, (iii) presence of mass transfer limitations to the catalytic reactions, due to the high temperature required [8].

* Corresponding author. Tel.: +39-6-49913378; fax: +39-6-490324.
E-mail address: piero.porta@uniromal.it (P. Porta).

1381-1169/01/$ – see front matter
PII: S1381-1169(01)00265-5

All these possible reaction pathways lower the selectivity to C_2-hydrocarbons and can lead to undesirable deactivation phenomena.

Even if the gas-phase reaction plays an important role in the overall process, the presence of the catalyst is fundamental. Methane dehydrogenates on the catalyst surface and produces methyl radicals, which can react over the surface or in the gas phase. The abstraction of a hydrogen atom is caused by an oxygen ion present on the surface of the catalyst, but many types of oxygen ions can occur (from O_2^- to O^{2-}), that is from the less to the most "basic" species. It is generally accepted that O^{2-} sites, that is surface oxygen species with sufficiently high binding energy, are decisive for enhancing the formation of methyl radicals and therefore of C_2-hydrocarbons instead of producing carbon oxides. On the contrary, more oxidizing and weakly bound ions like for instance O_2^-, O_2^{2-}, O^-, are supposed to favor the formations of carbon oxides [9].

Since metal oxides promoted with lanthanide oxides are active and selective catalysts in methane coupling [10], it seemed of interest to study perovskite-type oxide materials where the promoter and metal are in the same framework. Perovskite-type oxides are indeed characterized by high mobility of both electrons and oxygen ions, which can make them suitable for the methane coupling reaction.

Perovskite oxides have general formula ABO_3, where the 12-coordinated A and 6-coordinated B sites are occupied by large ($r_A > 0.90$ Å) and smaller ions ($r_B > 0.51$ Å), respectively. Due to the great stability of the perovskite structure a large number of metals can occupy the A and the B sites provided that the so-called "tolerance factor" t [$t = (r_A + r_O)/\sqrt{2}(r_B + r_O)$] is in the range 0.8–1.0 [11,12]. Moreover, the perovskite composition can be widely changed by substituting either or both the A and B site cations with other metals with different oxidation state. In this case, formation of structural defects such as anionic or cationic vacancies arises in order to maintain the electroneutrality of the compound. For instance, upon substitution of A^{3+} and/or B^{3+} cations by a metal preferentially stable in an oxidation state lower than +3, the charge compensation is achieved, when possible, by a decrease in the oxygen content of the perovskite with the eventual appearance of oxygen vacancies. This occurrence strongly affects the redox properties of the catalyst.

A perovskite material like $LaAlO_3$ (La^{3+} and Al^{3+} occupying the A and the B lattice sites, respectively) contains strongly bound oxygen species and thus, appears a suitable catalyst for the methane coupling reaction. An amorphous material of this composition has been recognized as a promising substance in the methane coupling reaction [13]. A higher activity and selectivity of the catalysts for the oxidative coupling of methane was obtained by proper cation substitution in perovskite-type oxides [14].

The partial substitution of lanthanum or aluminum, in $LaAlO_3$, with alkali or alkali-earth ions was undertaken in the present investigation with the aim of varying the strength of the oxygen-lattice bonds. The structural, adsorptive (towards oxygen) and catalytic (towards methane coupling reaction) properties of $La_{1-x}M_xAlO_3$ (M = Na, K, Ca, Ba) and $LaAl_{1-x}M_xO_3$ (M = Li, Mg) perovskite-type solid solutions are reported.

2. Experimental

$La_{1-x}M_xAlO_3$ (M = Na, K, Ca, Ba) and $LaAl_{1-x}M_xO_3$ (M = Li, Mg) catalysts were prepared from citrate precursors [15,16]. A concentrated solution of the metal nitrates was mixed with an aqueous solution of citric acid, by fixing at unity the molar ratio of citric acid to the metal cations. Water was evaporated from the mixed solution at 80°C until a viscous gel was obtained. The gel was kept at 100°C overnight, ground and finally calcined at 800°C for 5 h.

Phase analysis, lattice parameters, and particle size determination were performed by XRD using a Philips PW 1729 diffractometer equipped with an IBM PS2 computer for data acquisition and analysis (software APD-Philips). Scans were taken with a 2θ step of 0.01° and using Ni-filtered Cu Kα radiation. Lattice parameters were evaluated from all reflections appearing in the range of 2θ = 20–60°, by means of the UNIT-CELL program [17]. Particle sizes were evaluated by means of the Scherrer equation $D = K\lambda/\beta \cos\theta$ after Warren's correction for instrumental broadening [18], where D is the mean crystallite diameter of the particles supposed spherical, K a constant equal to 0.9, λ the wavelength of the X-ray used, β the effective line width of the X-ray reflection under observation, calculated by the expression $\beta^2 = B^2 - b^2$,

where B is the full width at half maximum (FWHM), β the instrumental broadening determined through the FWHM of the X-ray reflection at $\theta = 14^\circ$ of SiO_2 having particles larger than 1000 Å, and θ the diffraction angle of the perovskite X-ray reflection ($\theta = 16.7^\circ$).

BET surface areas were measured by krypton or nitrogen adsorption at –196°C, in a volumetric all glass apparatus.

Catalytic tests were carried out in a tubular continuous flow reactor, 1 cm o.d., employing 0.1 g of catalyst and a flow of methane/oxygen (5/1) diluted in helium (reactants/total flow = 0.4). The gases were purified and dehydrated by means of suitable filters and their flows were regulated by means of MKS electronic mass flow controllers. The reaction was investigated in the range 600–750°C after an in situ pre-treatment of the catalysts, in a flow of oxygen (20%) in helium at 600°C for 1 h. The reaction was then carried out starting from 600°C, increasing stepwise the temperature and analyzing the reaction mixture in steady state conditions at every pre-determined temperature. The reaction mixture was analyzed by means of Perkin-Elmer Autosystem gas chromatograph, equipped with Plot-Q capillary columns. Since a rapid deactivation was always observed on these catalysts, reactivation treatments were performed in each run during heating from previous to the next selected temperature by interrupting the methane flow, that is allowing only oxygen and helium to flow over the catalyst.

The adsorptive properties of the catalysts towards oxygen were studied by means of temperature programmed desorption (TPD) experiments. Oxygen adsorption was carried out in a tubular reactor on samples of 0.06 g, after the same oxidative pre-treatment used in the activity determination experiments, by cooling down the samples in the same oxidant flow to room temperature and allowing equilibration in pure oxygen flow at such a temperature for 3 h. Then desorption was carried out in a flow of helium as carrier gas at a heating rate of 4–16°C/min.

In every experiment, the flows of the gases, dried and purified with suitable filters and with a liquid nitrogen trap, were regulated with Brooks electronic mass flow controllers, and the peaks were detected by means of a HWD detector.

3. Results and discussion

Table 1 reports the chemical formula and the values of unit-cell parameter, crystallite size, specific surface area for all the catalysts.

Fig. 1 shows the XRD patterns for all the catalysts. All samples exhibited a rhombohedral perovskite structure with $R\bar{3}m$ space group [19]. Only for $La_{0.9}Ba_{0.1}AlO_3$ the XRD pattern revealed the presence of small amount of $BaCO_3$ in addition to the perovskite phase.

The values of the mean crystallite diameter, D, reflect the trend of crystallinity observed on the relative XRD patterns, and almost agree with the opposite trend exhibited by the specific surface area (SA).

The unit-cell volume, V, of all the substituted perovskites is lower than that of pure $LaAlO_3$. Since the ionic radius values of 12-coordinated Na^+ (1.39 Å), K^+ (1.64 Å) and Ba^{2+} (1.61 Å) are higher than that of La^{3+} (1.36 Å) [20], and the ionic radius values of the octahedral Li^+ (0.76 Å) and Mg^{2+} (0.72 Å) are also higher than that of Al^{3+} (0.535 Å) [20], the observed lattice shrinkage is likely due to the presence of oxygen vacancies compensating the positive charge defectivity. The chemical formula of the $La_{1-x}M_xAlO_3$

Table 1
Chemical formulae for each perovskite catalyst[a]

Catalyst	a	c (Å)	V (Å^3)	D (Å)	SA (m^2 g^{-1})	MC (%)	SC_2 (%)
$LaAlO_3$	5.367	13.134	327.56	1100	4.3	16.3	57.7
$LaAl_{0.9}Li_{0.1}O_3$	5.410	12.880	325.98	653	10	17.0	65.3
$LaAl_{0.9}Mg_{0.1}O_3$	5.370	13.110	314.14	542	14	18.4	64.7
$La_{0.9}Na_{0.1}AlO_3$	5.358	14.123	326.31	530	14	14.6	58.5
$La_{0.9}K_{0.1}AlO_3$	5.361	13.117	326.53	950	15	16.6	59.6
$La_{0.9}Ca_{0.1}AlO_3$	5.351	13.144	325.88	430	16	14.5	55.9
$La_{0.9}Ba_{0.1}AlO_3$	5.365	13.101	326.60	430	21	16.3	54.0

[a] SA: specific surface area; D: crystallite size; MC: methane conversion; SC_2: selectivity to C_2-hydrocarbons obtained at 750°C.

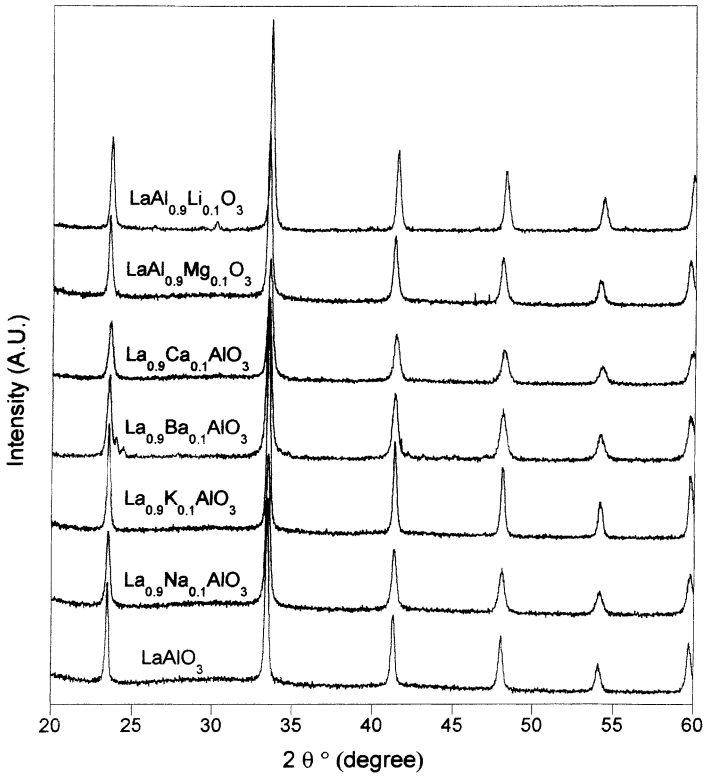

Fig. 1. X-ray diffraction patterns for the $La_{1-x}M_xAlO_3$ (M = Na, K, Ca, Ba) and $LaAl_{1-x}M_xO_3$ (M = Li, Mg) catalysts.

and $LaAl_{1-x}M_xO_3$ samples should therefore be written as $La_{1-x}M_xAlO_{3-\delta}$ and $LaAl_{1-x}M_xO_{3-\delta}$, where δ indicates the amount of the oxygen defectivity.

The results of the catalytic activity and selectivity to C_2-hydrocarbons at 750°C of the examined catalysts are summarized in Table 1 and the trends of the various products with the reaction temperature are shown in Fig. 2a,b,c,d. The substitution of Al by Li and Mg in the octahedral B sites of the ABO_3 perovskite structure seems to be beneficial, either for an improvement of about 10% of the activity or for an enhancement of 15% of the selectivity to C_2 in comparison with pure $LaAlO_3$. The differences in catalytic activity and selectivity between pure $LaAlO_3$ and the substituted $LaAl_{0.9}Li_{0.1}O_3$ and $LaAl_{0.9}Mg_{0.1}O_3$ perovskites are much more marked at lower temperature, for example, at 700°C.

Figs. 3–5 show the oxidation reactions of the products obtained in the oxidative methane coupling. Since in the reaction of methane coupling the great part of oxygen is consumed by methane itself, the experiments were performed at low content of oxygen (oxidisable compound/oxygen molar ratio = 10/1), with the aim to better understand the reactions that may occur between the oxygen not consumed by methane and the products of partial oxidation of methane. We observed the following features:

1. CO is easily oxidized to carbon dioxide under methane coupling conditions (Fig. 3).
2. Ethane oxidation (Fig. 4a and b) yielded ethylene, very small amounts of carbon oxides and methane. Therefore, the production of ethylene in methane coupling (Fig. 2d) is most probably due to the oxidation of ethane.
3. Ethylene oxidation (Fig. 5a and b) gives small amounts of carbon oxides in addition to small, but not negligible, amounts of ethane and methane.
4. In many experiments, the production of carbonaceous species on the catalyst surface has been

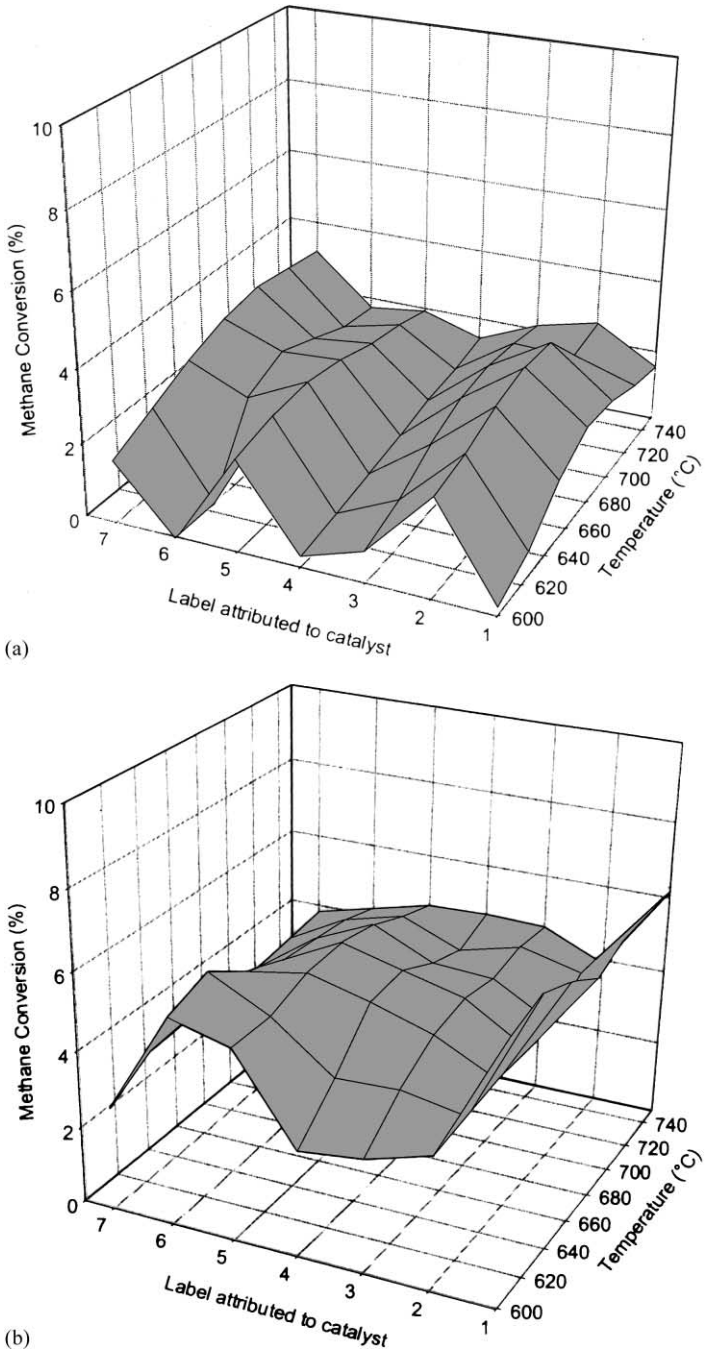

Fig. 2. Methane conversion (%) to (a) CO, (b) CO_2, (c) C_2H_6, and (d) C_2H_4. Ratio $CH_4/O_2 = 5$; ratio reactants/total flow = 1/2.5. Amount of catalyst: 0.1 g. In any diagram the term "label attributed to catalysts" represents: (1) $La_{0.9}Ba_{0.1}AlO_3$; (2) $La_{0.9}Ca_{0.1}AlO_3$; (3) $La_{0.9}K_{0.1}AlO_3$; (4) $La_{0.9}Na_{0.1}AlO_3$; (5) $LaAl_{0.9}Mg_{0.1}O_3$; (6) $LaAl_{0.9}Li_{0.1}O_3$; (7) $LaAlO_3$.

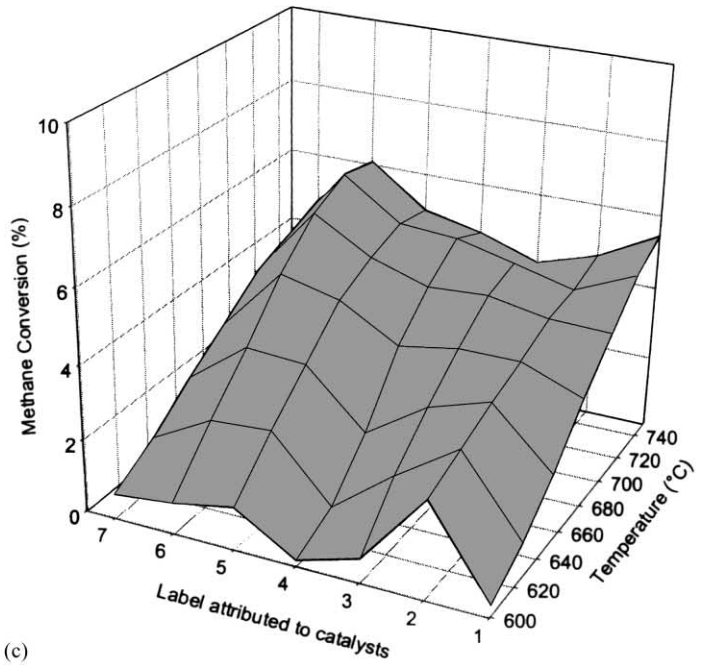

(c)

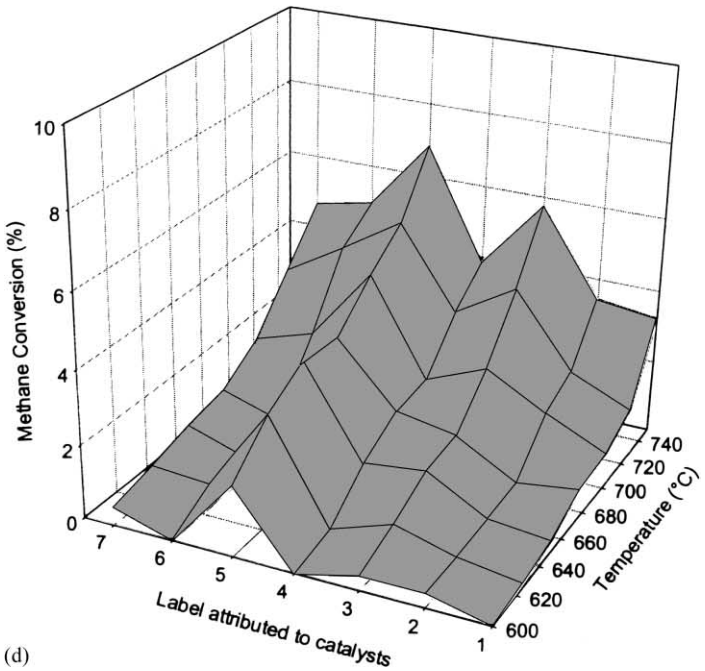

(d)

Fig. 2. (*Continued*).

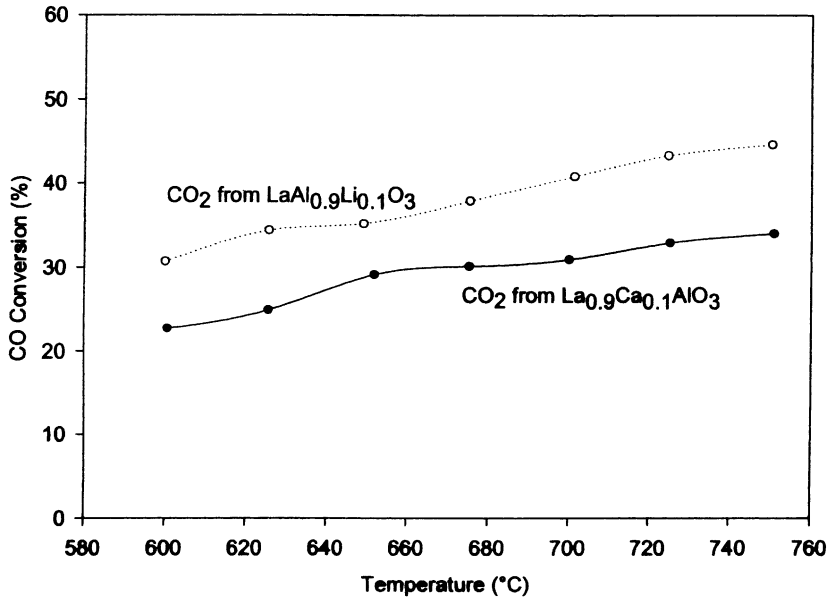

Fig. 3. CO conversion (%) to CO_2 during oxidative reactions in conditions of oxygen deficient mixtures.

revealed especially at high temperature. These species are responsible for the catalyst deactivation shown in Fig. 6 for $La_{0.9}K_{0.1}AlO_3$ as an example.

Points (1), (2) and (3) suggest that the methane coupling and oxidation reaction to carbon oxides occur in the same time on different active sites, i.e. on different type of oxygen. Therefore, a very complicated reaction pathway can be supposed (Fig. 7).

The values of conversion to carbon oxides and to C_2-hydrocarbons obtained during methane coupling can be affected by diffusion control problems because of the high temperatures of reaction.

Since the porosity of $LaAlO_3$ and of other derived materials is low, intraphase diffusion should not be important, but interphase diffusion may be rate limiting. A common method for testing the existence of diffusion limitations consists in diluting the reactants mixture in the carrier gas. Experiments were therefore carried out by using the same methane/oxygen ratio and reducing approximately three times their partial pressures.

The results, shown in Fig. 8, demonstrate that the methane fraction converted to CO and CO_2 is drastically reduced, whereas the amount of methane converted to C_2-hydrocarbons does not change appreciably. Oxygen diffusion from the gas phase to the catalyst surface strongly affects the total oxidation reaction, whereas it seems not important for the formation of C_2-hydrocarbons. This may confirm that two distinct reactions, leading to carbon oxides and to C_2-hydrocarbons, occur on the catalyst surface.

The adsorptive properties of the catalysts towards oxygen are important in this type of reactions, oxygen species with enhanced basic properties being considered decisive for dehydrogenative coupling. The TPD patterns of adsorbed O_2 on pure and substituted perovskites are shown in Fig. 9.

Two types of oxygen species have been reported [21] as responsible for the TPD peaks at different temperatures.

TPD spectra (Fig. 9) display a first small and broad peak centered at about 350–450°C, and corresponding to an amount of adsorbed oxygen varying from 3×10^{-7} to 6×10^{-7} mol m^{-2} of catalyst for lanthanum substituted perovskites, to 2.6×10^{-5} mol m^{-2} for $LaAl_{0.9}Li_{0.1}O_3$, and to 3.2×10^{-5} mol m^{-2} for $LaAl_{0.9}Mg_{0.1}O_3$. The low temperature peak corresponds to oxygen surface species weakly bound to the lattice [22,23].

The second peak, when present, is placed at very high temperatures, and in some instances it is far from the end, even at 900°C. This testifies the strength of

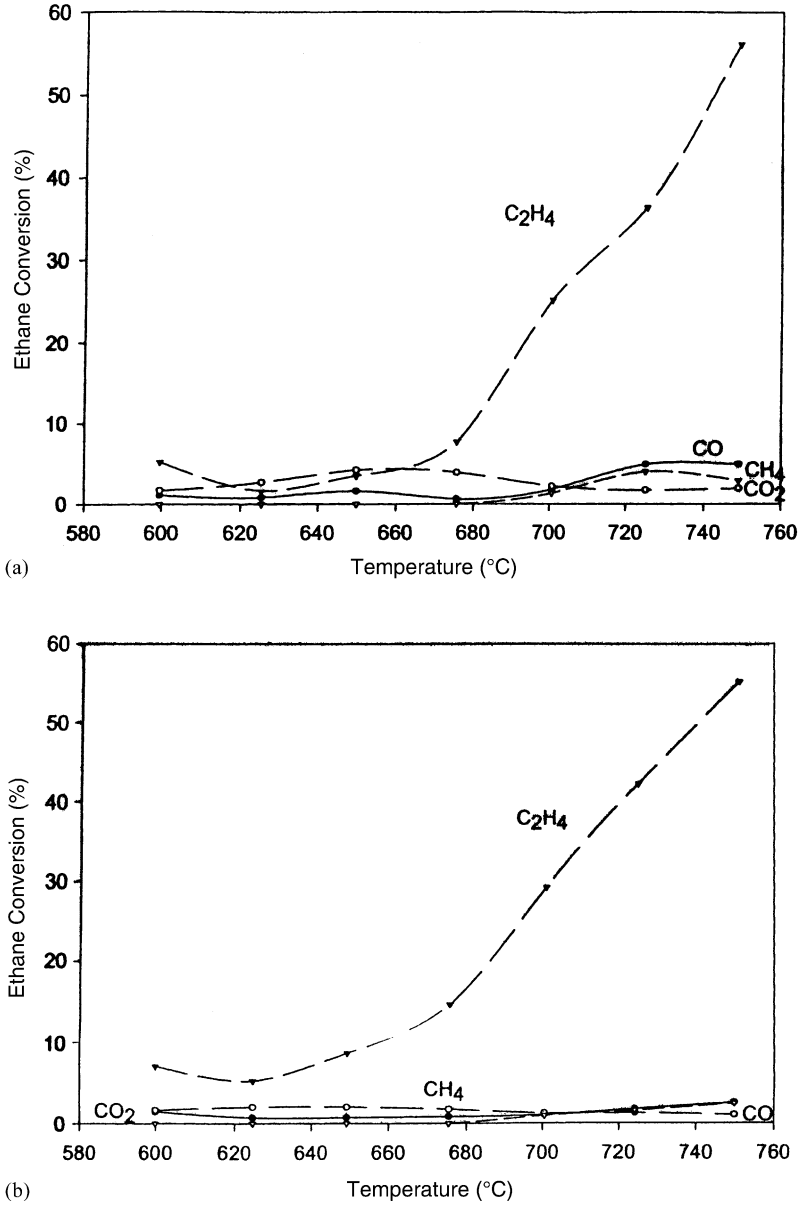

Fig. 4. Ethane conversion (%) to C_2H_4, CO, CO_2, and CH_4 during oxidative reactions in conditions of oxygen deficient mixtures on (a) $La_{0.9}K_{0.1}AlO_3$ and (b) $LaAl_{0.9}Mg_{0.1}O_3$.

the bonds of this type of oxygen to the lattice. The high temperature peak is nearly absent in the TPD spectra of aluminum substituted perovskites, which are the most active and selective to C_2-hydrocarbons. This suggests that the presence of Li and Mg increases the bond strength of lattice oxygen.

Two types of oxygen surface species, one less strongly bound to lattice and leading to carbon oxides, and one more strongly bound and leading to C_2-hydrocarbons, are present.

By representing the first type of active oxygen by O^-, we suggest that such a species is sufficiently

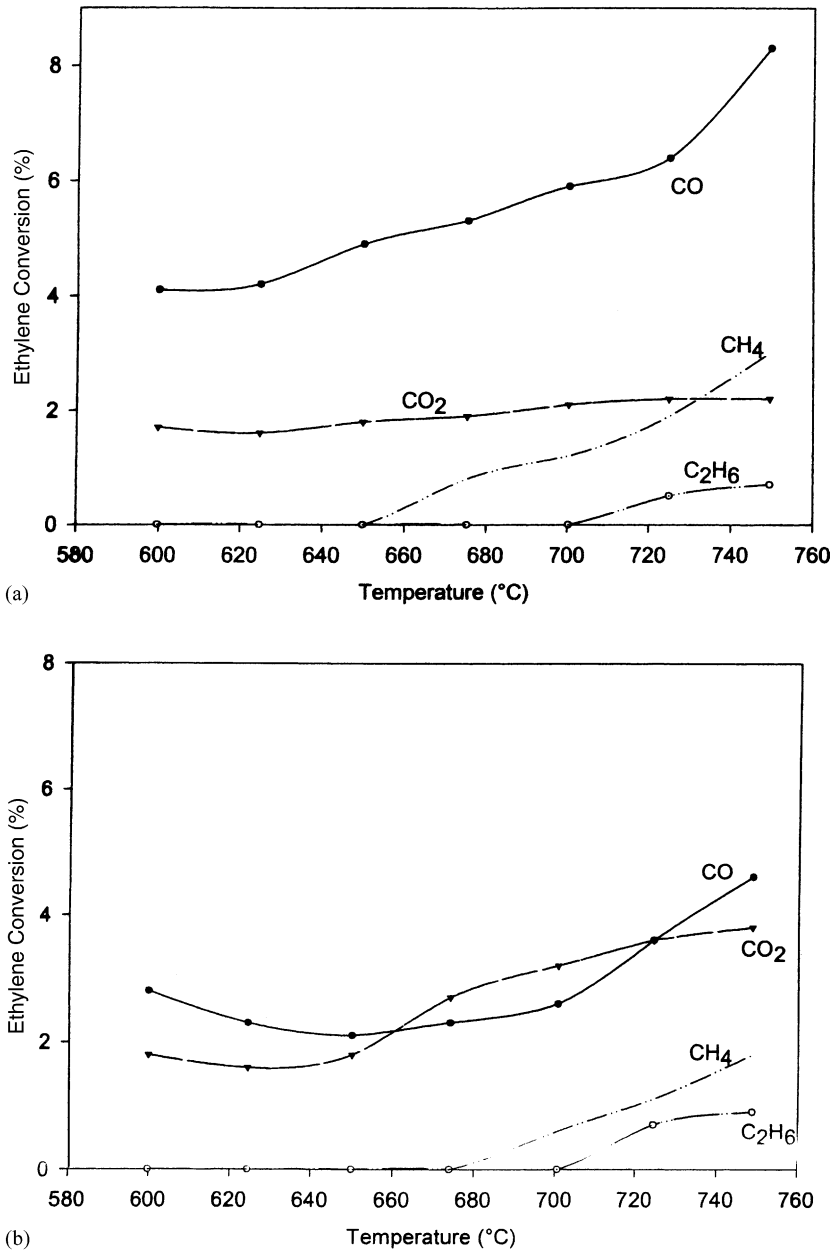

Fig. 5. Ethylene conversion (%) to C_2H_6, CO, CO_2, and CH_4 during oxidative reactions in conditions of oxygen deficient mixtures on (a) $La_{0.9}Ca_{0.1}AlO_3$ and (b) $LaAl_{0.9}Li_{0.1}O_3$.

"electrophilic" to attack the carbon atom of methane, according to the following reaction where the formation of an adsorbed methanol molecule is hypothesized:

$$CH_4 + O^- \rightarrow H_4C\text{–}O^- \rightarrow H_3C\text{–}OH + e^-$$

The adsorbed methanol molecule is most probably the first intermediate of a series, which leads at the

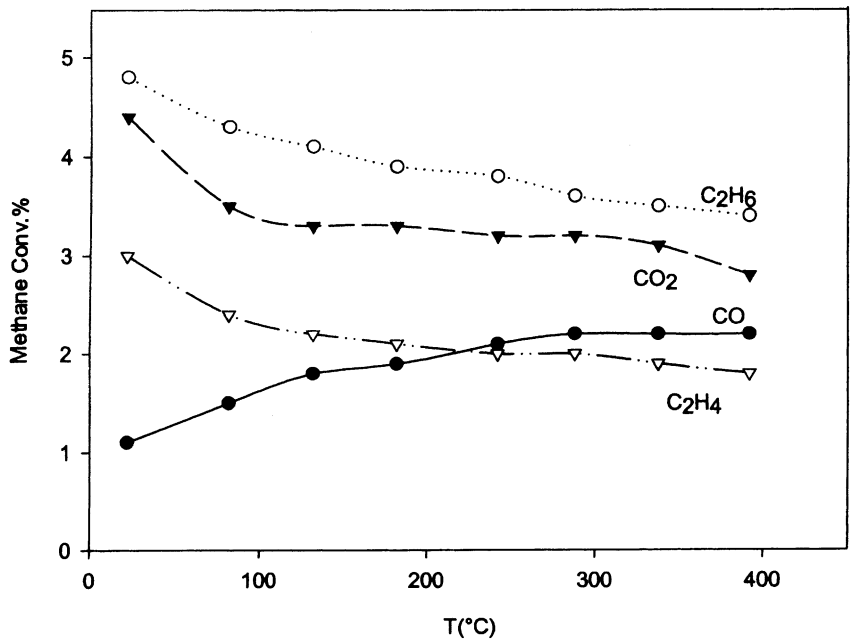

Fig. 6. Methane conversion (%) in function of time at 700°C, to test deactivation on $La_{0.9}K_{0.1}AlO_3$.

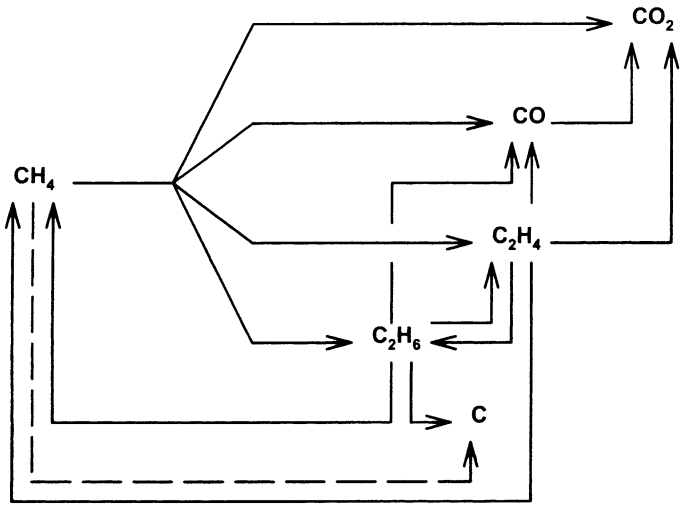

Fig. 7. Pattern of the possible reactions occurring in the conditions employed during methane coupling.

end to carbon oxides and water. The electron can be attracted by a metal ion near to an oxygen vacancy and made available to gaseous oxygen for its reduction

$$\tfrac{1}{2}O_2 + e^- \rightarrow O^-$$

The diffusion of gaseous oxygen from the gas phase to the catalyst surface, prior to the above reaction, would be the rate determining step in the series of steps eventually leading to complete combustion, as suggested above.

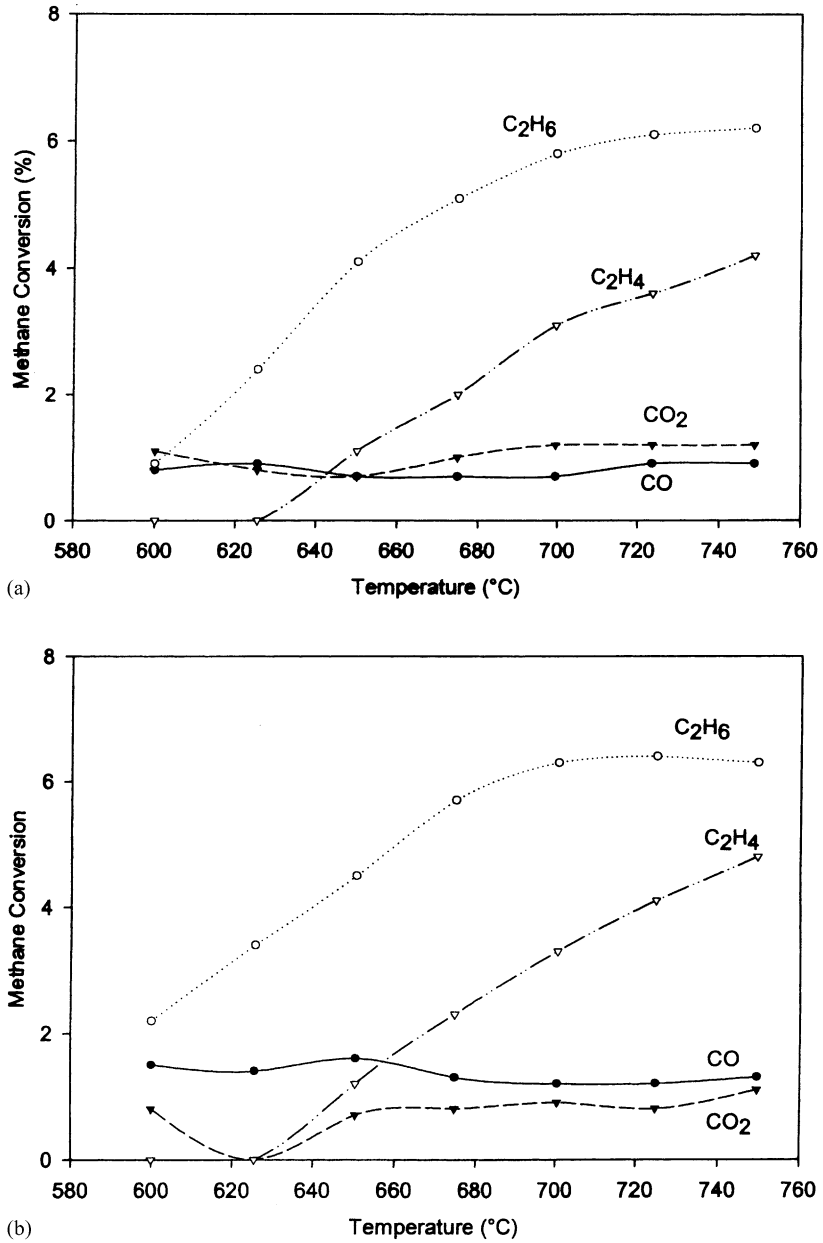

Fig. 8. Methane conversion (%) to CO, CO_2, C_2H_6 and C_2H_4. Ratio $CH_4/O_2 = 5$; ratio reactants/total flow = 1/4.2: (a) $La_{0.9}K_{0.1}AlO_3$; (b) $LaAl_{0.9}Li_{0.1}O_3$.

A different type of oxygen may be suggested for the formation of C_2-hydrocarbons, for instance the O^{2-} species, which is electron rich (therefore "nucleophilic") and can attack the hydrogen atom

$$CH_4 + O^{2-} \rightarrow CH_3^{\bullet} + OH^- + e^-$$

Methyl radicals can dimerize giving ethane, and two hydroxyls give a water molecule, an O^{2-} and an anionic vacancy. The electrons produced can be at-

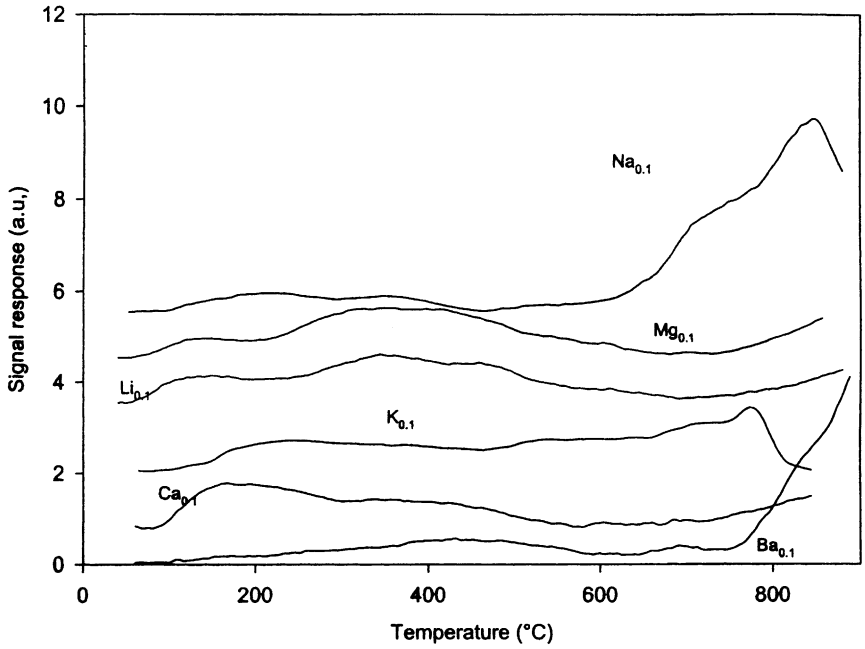

Fig. 9. Temperature programmed desorption profiles obtained with oxygen adsorbed in continuous flow at room temperature. Amount of catalyst: 0.06 g.

tracted by a metal ion near to an oxygen vacancy and made available to gaseous oxygen for its reductive chemisorption

$$\tfrac{1}{2}O_2 + 2e^- \rightarrow O^{2-}$$

The possibility of realizing one or the other of the two mechanisms is connected to a number of factors, namely, the reducibility of the metal ion (especially the octahedrally coordinated B-type metal ion), the presence of oxygen and cation vacancies (eventually introduced by partial substitution of metal ions), and the presence of structural distortions introduced by the metal substitution.

In $LaAlO_3$ neither lanthanum nor aluminum shows appreciable redox properties and this entails that a relevant amount of firmly bound oxygen species can be present. An increase of vacancies with temperature makes possible a certain mobility of electrons, and a reactivity (at high temperature) addressed toward the oxidative coupling.

Two opposite effects can be supposed at this stage: (i) the introduction of less charged ions causes the presence on the surface of a lower number of oxygen species strongly bound to the lattice; (ii) the oxygen species are bound to metal ions with more basic character; thus, having a greater ability to nucleophilic attack towards methane. During the reaction, movement of the charges enables an equilibrium also of the type

$$2O^{2-} \rightleftarrows {O_2}^{2-} + 2e^-$$

This is a source of oxygen species less negatively charged, not stable at these high temperatures, and therefore easily available on the surface and able to activate methane towards the formation of carbon oxides. Probably these species cannot be replaced so easily by gaseous oxygen and this hypothesis could explain the control of oxygen diffusion from gas phase to the surface for the total oxidation of methane.

4. Conclusions

All the catalysts exhibit the perovskite structure. Due to charge compensation, the substitution of trivalent La and Al ions by metals with lower oxidation state produces oxygen vacancies that induce a reactivity of these catalysts, activating methane towards total or partial oxidation.

The presence of two types of oxygen species is confirmed by means of TPD experiments, which demonstrate that on the studied perovskites a meaningful fraction of oxygen species desorbs at high temperatures and is strongly bound to the surface.

The substitution of B-type ions either with monovalent or divalent ions seems to be beneficial for the catalytic activity and the selectivity towards C_2 formation due to the increased strength of the bonds between oxygen and lattice.

The partial and total oxidations seem to proceed along distinct pathways through a series of intermediate steps: CO is easily oxidized to CO_2 and C_2H_6 is substantially oxidized to C_2H_4. The conversion of ethane demonstrates that ethylene is almost completely produced by ethane oxidative dehydrogenation. However, the yield of ethylene is decreased by consecutive cracking and oxidation. These reactions occur, however, only to a little extent.

The selectivity to C_2-hydrocarbons increases by diluting the reactant mixture and decreasing their contact time on the catalyst. This result can be ascribed to the presence of external mass transfer limitations in total oxidation.

References

[1] J.M. Fox, Catal. Rev. Sci. Eng. 35 (1993) 169.
[2] J.L.G. Fierro, Catal. Lett. 22 (1993) 67.
[3] J.H. Lunsford, Catal. Today 63 (2000) 165.
[4] G. Lu, S. Shen, R. Wang, Catal. Today 30 (1996) 41.
[5] G.E. Keller, M.M. Bhasin, J. Catal. 73 (1982) 9.
[6] D.J. Driscoll, K.D. Campbell, J.H. Lunsford, Adv. Catal. 35 (1987) 139.
[7] G.S. Lane, E.E. Wolf, J. Catal. 113 (1988) 144.
[8] D. Wolf, M. Höhenberger, M. Baerns, Ind. Chem. Eng. Res. 36 (1997) 3345.
[9] O.V. Krylov, Catal. Today 18 (1993) 209.
[10] K. Otsuka, K. Jinno, Inorg. Chim. Acta 121 (1986) 237.
[11] L.G. Tejuca, J.L.G. Fierro (Eds.), Properties and Applications of Perovskite-Type Oxides, Marcel Dekker, New York, 1993.
[12] V.M. Goldschmidt, Akad. Oslo. J. Mater. Natur. 2 (1926) 7.
[13] H. Imai, T. Tagawa, N. Kamide, J. Catal. 106 (1987) 399.
[14] H. Nagamoto, K. Amanuma, H. Nobutomo, H. Inoue, Chem. Lett. (1988) 237.
[15] Belg. Pat. 735,476, (15 September 1969).
[16] B. Delmon, J. Droguest, in W.H. Fuhn (Ed.), in: Proceedings of the 2nd International Conference on Fine Particles, The Electrochemical Society, 1973, p. 242.
[17] T.J.B. Holland, S.A.T. Redfern, J. Appl. Crystallogr. 30 (1997) 84.
[18] H.P. Klug, L.E. Alexander, X-ray Diffraction Procedures for Polycrystalline and Amorphous Materials, Wiley, London, 1962, p. 492.
[19] Powder Diffraction File, Inorganic Volume, File 31-22, Am. Soc. Testing Materials, Philadelphia, 1967.
[20] R.D. Shannon, Acta Crystallogr. Sect. A 32 (1976) 751.
[21] T. Seiyama, N. Yamazoe, K. Eguchi, Ind. Eng. Chem. Prod. Res. Dev. 24 (1985) 19.
[22] L. Marchetti, L. Forni, Appl. Catal. B: Environ. 15 (1998) 179.
[23] H. Arai, T. Yamada, K. Eguchi, T. Seiyama, Appl. Catal. 26 (1986) 265.